

# Characterization of a Radical Intermediate in Lipoyl Cofactor Biosynthesis

Nicholas D. Lanz,<sup>‡</sup> Justin M. Rectenwald,<sup>†</sup> Bo Wang,<sup>†</sup> Elizabeth S. Kakar,<sup>‡</sup> Tatiana N. Laremore,<sup>§</sup> Squire J. Booker,<sup>\*,†,‡</sup> and Alexey Silakov<sup>\*,†</sup>

Departments of <sup>†</sup>Chemistry and <sup>‡</sup>Biochemistry and Molecular Biology and <sup>§</sup>The Huck Institutes of the Life Sciences, The Pennsylvania State University, University Park, Pennsylvania 16802, United States

**S** Supporting Information

**ABSTRACT:** Lipoyl synthase (LipA) catalyzes the final step in the biosynthesis of the lipoyl cofactor, the insertion of two sulfur atoms at C6 and C8 of an *n*-octanoyl chain. LipA is a member of the radical *S*-adenosylmethionine (SAM) superfamily of enzymes and uses two [4Fe–4S] clusters to catalyze its transformation. One cluster binds in contact with SAM and donates the requisite electron for the reductive cleavage of SAM to generate two 5'-deoxyadenosyl 5'-radicals, which abstract hydrogen atoms from C6 and C8 of the substrate. By contrast, the second, auxiliary [4Fe–4S] cluster, has been hypothesized to serve as the sulfur donor in the reaction. Such a sacrificial role for an iron–sulfur cluster during catalysis has not been universally accepted. Use of a conjugated 2,4-hexadienoyl-containing substrate analogue has allowed the substrate radical to be trapped and characterized by continuous-wave and pulsed electron paramagnetic resonance methods. Here we report the observation of a <sup>57</sup>Fe hyperfine coupling interaction with the paramagnetic signal, which indicates that the iron–sulfur cluster of LipA and its substrate are within bonding distance.

Lipoyl synthase (LipA) catalyzes the final step in the *de novo* biosynthesis of the lipoyl cofactor, which is the insertion of sulfur atoms at C6 and C8 of an *n*-octanoyl chain attached in an amide linkage to a target lysine residue of a lipoyl carrier protein (LCP) (Figure 1A). The transformation is functionally analogous to those of the many iron-requiring enzymes that activate dioxygen for hydroxylation of substrates;<sup>1</sup> however, no similar mechanisms for sulfur insertion exist. Indeed, LipA belongs to the radical *S*-adenosylmethionine (SAM) superfamily of enzymes, which catalyze a reductive cleavage of SAM to methionine and a 5'-deoxyadenosyl 5'-radical (5'-dA•), a potent oxidant.<sup>2</sup> In almost all radical SAM (RS) enzymes, the role of the 5'-dA• is to abstract a hydrogen atom (H•) from an enzyme-bound substrate to generate a substrate radical intermediate. The identity of the substrate and the fate of the substrate radical intermediate distinguishes over 40 distinct reaction types found in the superfamily, such as, among others, methylation, sulfhydrylation, and methylthiolation of unactivated carbon centers as well as dehydrogenation, 1,2-cross migration, epimerization, thioether formation, and a variety of complex fragmentations and/or rearrangements.<sup>3</sup>

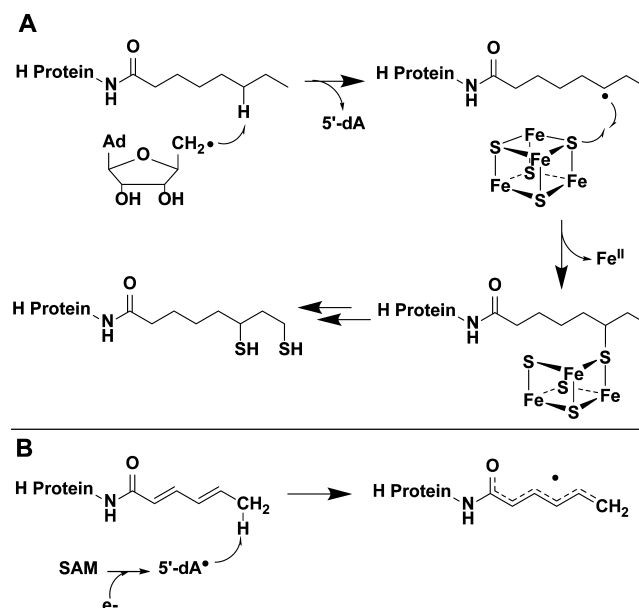


**Figure 1.** Proposed mechanism of the LipA first half-reaction of (A). Abstraction of an H• from C6 of the octanoyl substrate results in a transient carbon-centered radical. Recombination with a bridging  $\mu_3$ -sulfido ion of the auxiliary cluster results in a stable cross-linked intermediate. Repetition of this process at C8 of the substrate results in the lipoylated H protein. The reaction using the 2,4-hexadienoyl-H protein substrate analogue (B) allows the substrate radical to be trapped and characterized.

The distinguishing feature of RS enzymes is a [4Fe–4S] cluster ligated by three cysteine residues found almost universally in a CX<sub>3</sub>CX<sub>2</sub>C motif.<sup>4</sup> The [4Fe–4S] cluster, when in its 1+ charge state, provides the requisite electron for the reductive cleavage of SAM to generate the 5'-dA•. All enzymes annotated as lipoyl synthases, however, harbor a second, strictly conserved, motif (CX<sub>5</sub>CX<sub>4</sub>C), in which the cysteines therein ligate a second, auxiliary, [4Fe–4S] cluster. In LipA, 2 equiv of the 5'-dA• are required to generate 1 equiv of the lipoyl cofactor, and the two 5'-dA• have been shown to abstract H• sequentially from C6 and then C8 of octanoyl chains attached to LCPs or to short peptide substrate surrogates.<sup>5</sup> Importantly, labeling studies indicate that the inserted sulfur atoms are both derived from LipA, itself,

Received: May 7, 2015

Published: September 21, 2015

raising the question as to the exact nature of the sulfur donor and the underlying chemistry that allows incorporation of sulfur into the organic substrate.<sup>6</sup>

Recent studies have provided evidence that the auxiliary [4Fe–4S] cluster does indeed provide the inserted sulfur atom and is concomitantly sacrificed during turnover.<sup>7</sup> When LipA from *Escherichia coli* (*Ec*) was incubated under turnover conditions with a peptide substrate and only 1 equiv of SAM and then subjected to gel-filtration chromatography to remove small molecules, the resulting protein was shown by Mössbauer spectroscopy to contain one [4Fe–4S] cluster, in which SAM or methionine was bound to its unique iron ion, and a [3Fe–4S] cluster bridged to the 6-mercaptooctanoyl intermediate through one of its  $\mu_3$ -sulfido ions. When additional SAM and dithionite were added to the sample, but with no additional substrate, formation of lipoic acid ensued with concomitant destruction of the [3Fe–4S] cluster and formation of various ferrous ion species and small amounts of [2Fe–2S] clusters. These studies suggest that in the first half of the reaction, the octanoyl–LCP becomes cross-linked to LipA through the auxiliary [4Fe–4S] cluster. Consistent with this assumption, the cross-link between the two proteins could survive various forms of anaerobic chromatography, but was degraded upon exposure to oxygen.<sup>7</sup>

More recently, a structure of lipoyl synthase from *Thermosynechococcus elongatus* was solved to 1.6 Å resolution.<sup>8</sup> The structure showed the presence of both Fe/S clusters, which were separated by an 18 Å channel that was suggested to contain the binding sites for the organic substrate and SAM. Interestingly, the auxiliary cluster contained four ligands, one of which was a serine. Although the substrate was not present, the authors of the study modeled in SAM and *N* $\epsilon$ -octanoyllysine methylamide as a substrate surrogate. In this model, the distance between C5' of SAM and C6 of the substrate was 4.4 Å, while the distance between C6 of the substrate and the nearest  $\mu_3$ -sulfido ion of the auxiliary cluster was 6.4 Å.

In this work, we report our study on a reaction of LipA with a substrate analogue, 2,4-hexadienoic acid, attached to the appropriate lysine residue of the *Ec* H protein of the glycine cleavage system (Figure 1B). Though two-carbons shorter than the physiological substrate, the analogue was deemed a suitable substrate to investigate the proximity of the generated substrate radical to the auxiliary Fe/S cluster, given that abstraction of H• at C6 occurs before abstraction of H• at C8. Our expectation was that upon abstraction of H• from C6 of the substrate by the 5'-dA•, a conjugated substrate radical would be formed that might be detected by electron paramagnetic resonance (EPR) spectroscopic methods (Figure 1B).

To establish that 2,4-hexadienoyl-H protein is a viable substrate for LipA, matrix-assisted laser desorption/ionization-time-of-flight (MALDI-TOF) and Fourier transform mass spectrometry (FTMS) were used to demonstrate that the protein can catalyze insertion of a single sulfur atom into it. In the MALDI-TOF spectrum, a 32-mass unit shift was observed for the H protein in 2 h reactions of LipA with the 2,4-hexadienoyl substrate in the presence of SAM and dithionite (DT) (Figure S1). This observation was confirmed with FTMS and FT-MS/MS of a chymotryptic digest of the reaction, which allows for determination of the exact amino acid undergoing modification. The FTMS spectrum indicated that a fraction of the peptide (VDLPEVGATVSAGDDCAVAESVKAASDIY) containing the modified lysine (shown in bold) was shifted in mass by 32 Da (Figures 2 and S2). The y and b ion series subsequently allowed

localization of the 32 Da modification to the target lysine residue containing the 2,4-hexadienoyl substrate (Figure S3).

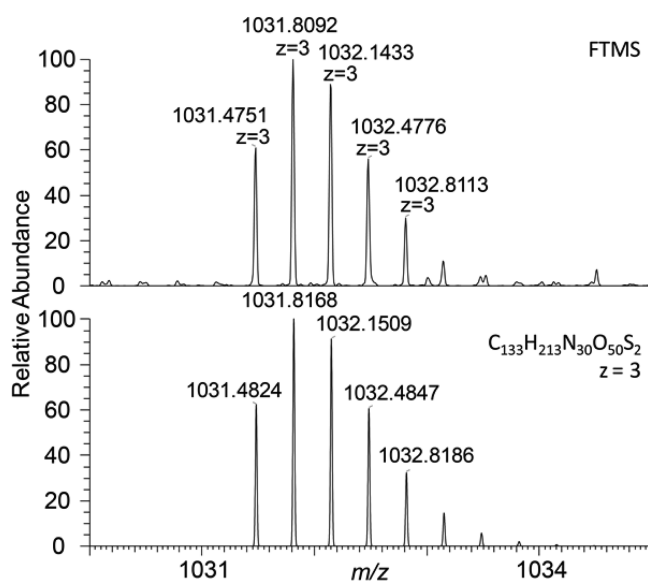


**Figure 2.** FT mass spectrum (top panel) and simulated isotopic distribution (bottom panel) of the chymotryptic peptide containing the modified lysine after insertion of one sulfur atom by LipA. Both Cys and 2,4-hexadienoyl sulfhydryls are carbamidomethylated. The observed  $m/z$  for the peptide containing the octanoyllysine is 1002.1446 ( $M + 3H$ ) for the unmodified substrate (Figure S2), whereas an  $m/z$  of 1031.8092 ( $M + 3H$ ) is detected after reaction with LipA, a mass shift of 88.9938 Da (carbamidomethyl = 57.0215, S = 31.9721).

To provide evidence for radical formation on the substrate analogue, a complex of LipA and 2,4-hexadienoyl-H protein was incubated at room temperature under turnover conditions for 2 min and then analyzed by EPR upon transferring to Q-band (2.8 mm O.D.; 1.8 mm I.D.) tubes and freeze-quenching in cryogenic isopentane. The sample reveals a spectrum containing a complex signal comprised of seven lines, consistent with it originating from a radical species strongly coupled to multiple protons (Figure 3a,b). The EPR signal is observable under a wide range of temperatures in continuous-wave (CW) mode as well as in pulse mode. Measurements at X-band (Figure 3a) and Q-band (Figure 3b) frequencies reveal spectra that are practically identical, indicating that the multiline pattern indeed originates from a strong hyperfine (HF) interaction with multiple  $^1\text{H}$  nuclei and that  $g$ -anisotropy is relatively small, which is typical for carbon-based radicals.

To better understand the spin distribution of the radical within the substrate, a specifically labeled substrate a completely deuterated terminal methyl group was generated to afford 6,6,6- $d_3$ -2,4-hexadienoyl-H protein ( $d_3$ -2,4-hexadienoyl). The radical species resulting from the reaction with this substrate exhibited a substantially simplified EPR spectrum as compared to that of the unlabeled substrate (Figure 3d). The change is attributed to a reduction of two  $^1\text{H}$  HF couplings due to the difference in the gyromagnetic ratios for  $^1\text{H}$  and  $^2\text{H}$  nuclei ( $g_n(^1\text{H})/g_n(^2\text{H}) = 6.51$ ). Q-band  $^2\text{H}$  hyperfine-sublevel correlation spectroscopy (HYSCORE) measurements confirmed the presence of two relatively isotropic  $^2\text{H}$  signals (Figure S4A). Additional  $^2\text{H}$ -labeling of the C5 position, 5,6,6,6- $d_4$ -2,4-hexadienoyl-H protein ( $d_4$ -2,4-hexadienoyl), revealed further simplification of the EPR spectrum and the appearance of

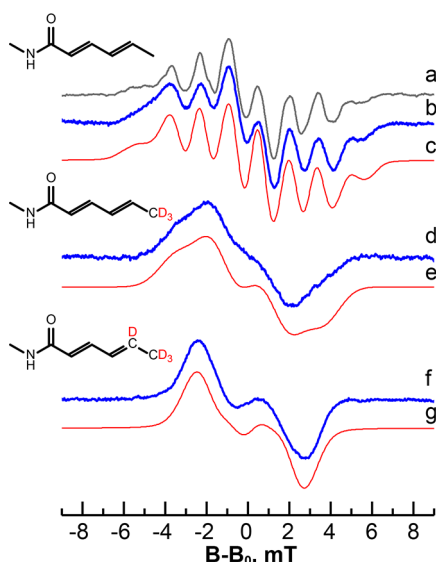


**Figure 3.** EPR spectra of the dithionite-reduced complex of LipA and 2,4-hexadienoyl-H protein (a,b,d,f) and corresponding simulation (c,e,g) using  $^1\text{H}$  HF coupling parameters from Table 1 and principal  $g$ -values  $g_{1,2,3} = 2.0053, 2.0054, 2.0058$ . (a,b) X- and Q-band EPR spectra of the unlabeled substrate and Q-band EPR spectrum of (d)  $d_3$ -2,4-hexadienoyl substrate and (f)  $d_4$ -2,4-hexadienoyl substrate. Q-band spectra were obtained by pseudomodulation of the absorption-like 2-pulse EPR spectrum. For convenience, the field axis is shifted by  $B_0 = 71.44 \nu_{\text{MW}}/2.0055$ . Experimental conditions: temperature, 25 K; microwave frequency, (a) 9.6228, (b) 34.2064, (d) 34.2732, and (f) 34.2770 GHz; (a) modulation amplitude, 2 G; conversion time, 40 ms, time constant, 40.96 ms; MW power, 2 mW; (b,d,f):  $T(\pi/2)$ , 16 ns;  $T(\pi)$ , 32 ns;  $\tau$ , 152 ns.

another, substantially anisotropic  $^2\text{H}$  signal in  $^2\text{H}$  HYSCORE spectra (Figure S4C).

**Table 1.**  $^1\text{H}$  Hyperfine Coupling Constants Used To Simulate EPR Spectrum Shown in Figure 3<sup>a</sup>

position	HFC	$A_1$ (MHz)	$A_2$ (MHz)	$A_3$ (MHz)
C6	H1 <sup>b,c</sup>	79 (3)	82 (3)	89 (3)
	H2 <sup>b,c</sup>	26 (3)	33 (1)	36 (3)
C5	H3 <sup>c</sup>	46 (5)	24 (5)	66 (5)
C4	H4	74 (2)	74 (2)	76 (2)
C3	H5	36 (5)	22 (5)	49 (5)
C2	H6	6 (3)	12 (2)	19 (5)

<sup>a</sup>Numbers in the brackets indicate the uncertainty in the units of the least significant digit. <sup>b</sup>Reduced by 6.51 in  $d_3$ -2,4-hexadienoyl substrate. <sup>c</sup>Reduced by 6.51 in  $d_4$ -2,4-hexadienoyl substrate.

Simulation of the resulting EPR spectra was achieved by inclusion of a total of six  $^1\text{H}$  nuclei (Table 1). Additionally, pulsed  $^1\text{H}$  ENDOR was performed to further detail the HF coupling constants (Figure S5). Table 1 shows the  $^1\text{H}$  HF coupling constants extracted from the simulation and the proposed assignment.

Based on the isotropic character of H1,H2 ( $\beta$ -proton-like) and a rhombic anisotropic character of H3 ( $\alpha$ -proton-like), we conclude that the radical is predominantly localized at C5 ( $\sim 65\%$ ). The nonequality of the H1 and H2 HFCs and the strong isotropic character of the H4 HFC indicate that the overall geometric and electronic structure of the 2,4-hexadienoyl group

is significantly perturbed from the expected planar arrangement and a conjugated radical (see Scheme S1 for the elaboration on the HFC assignment and spin distribution characterization).

The optimum temperature for observing the radical signal ( $\sim 25$ – $35$  K) is considerably lower than what is typical for pure organic radicals (70–100 K). Such an unusual temperature behavior could arise from an electron spin–spin interaction with a [4Fe–4S] cluster, which would also explain the observed perturbation of the structure of the substrate radical.

The proximity of the substrate radical to the [4Fe–4S] cluster was determined by analysis of  $^{57}\text{Fe}$  hyperfine interactions by Q-band HYSCORE<sup>9</sup> from LipA overproduced in minimal medium supplemented with  $^{57}\text{FeSO}_4$ . The measurements performed at the magnetic field corresponding to the maximum absorption reveal broad crosspeaks on an antidiagonal line centered at the Larmor frequency of  $^{57}\text{Fe}$  ( $\nu_L = 1.68$  MHz at 1220 mT, Figures S4 and 4). The origin of the ridges was clarified by comparing

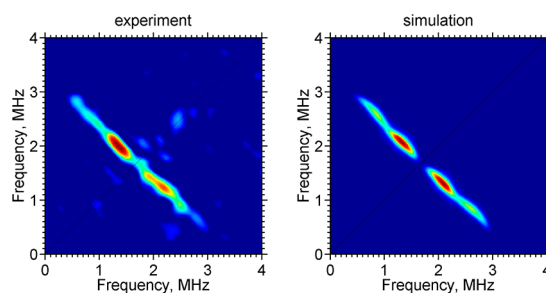


**Figure 4.** Q-band HYSCORE spectrum of DT-reduced  $^{57}\text{Fe}$ -enriched LipA in complex with 2,4-hexadienoyl-H protein (left) as compared with a simulation accounting for two  $^{57}\text{Fe}$  nuclei with HF couplings constants shown in Table 2. Only the (++) quadrant is shown. Experimental conditions: temperature, 25 K; magnetic field, 1219 mT;  $T(\pi/2)$ , 16 ns;  $\tau$ , 132 ns; microwave frequency, 34.165 GHz.

HYSCORE spectra of the  $^{57}\text{Fe}$ -labeled sample with those obtained with unlabeled LipA measured under the exact same conditions (Figure S6). The broad crosspeak on the antidiagonal line is only present in the HYSCORE spectrum of the  $^{57}\text{Fe}$ -enriched sample. Therefore, we can unambiguously attribute this signal to  $^{57}\text{Fe}$  nuclei in the vicinity of the radical.

To extract corresponding hyperfine coupling constants, a simulation was performed using in-house simulation programs (Figure 4). We note that the  $^{57}\text{Fe}$  signal cannot be simulated by accounting for only one interacting  $^{57}\text{Fe}$  nucleus, because the HF anisotropy necessary to reproduce the broadness of the ridge would considerably shift the simulated ridges upward in frequency away from the observed signals (Figure S7). Therefore, the HYSCORE spectra were interpreted using two  $^{57}\text{Fe}$  HF couplings of a relatively isotropic nature (Table 2). In the simulation we assume that all orientations in the “powder” pattern are excited.

The nature of the observed radical is unambiguous. The observed multiline EPR spectrum originating from multiple strong  $^1\text{H}$  hyperfine couplings is indicative of a radical species

**Table 2.**  $^{57}\text{Fe}$  HF Coupling Constants Used for the Simulation of the HYSCORE Spectrum Shown in Figure 4

nuc	$A_1$ (MHz)	$A_2$ (MHz)	$A_3$ (MHz)
$^{57}\text{Fe}_1$	1.2	1.4	2.5
$^{57}\text{Fe}_2$	1.3	1.0	0.1

located on the conjugated 2,4-hexadienoyl side chain. Measurements of the LipA protein in the absence of substrate reveal no such signal (data not shown). Based on the set of HF couplings extracted (Table 1), we conclude that the majority of spin density is located on C5 (~0.65) and to a lesser extent on C3.

We note, however, that DFT calculations performed for an isolated 2,4-hexadienoyl group show almost complete delocalization of the unpaired spin density over this moiety (Figure S8), resulting in hyperfine couplings much smaller than what has been deduced experimentally (Table 1). Therefore, the electronic structure of this side chain must be significantly perturbed, resulting in a redistribution of spin density. Based on the values of the HF couplings obtained, we suggest that C4 and C6 are strongly perturbed by an interaction with the  $[4\text{Fe}-4\text{S}]^{2+}$  cluster (see discussion in the SI).

In our HYSCORE experiments, we were able to resolve two  $^{57}\text{Fe}$  HF couplings, although it is possible that each obtained coupling is due to a pair of equivalent irons, as valence delocalization typically takes place for at least one of the two  $\text{Fe}^{\text{II}}-\text{Fe}^{\text{III}}$  pairs in  $[4\text{Fe}-4\text{S}]^{2+}$  clusters. These interactions have substantial isotropic character, which should not be the case if only a through-space dipolar magnetic interaction takes place. Therefore, a direct exchange interaction between the  $[4\text{Fe}-4\text{S}]$  cluster and the radical must exist that would induce isotropic  $^{57}\text{Fe}$  HF interactions.

Using a formulation of an exchange coupling mechanism for an unpaired electron coupled to a formally diamagnetic  $[4\text{Fe}-4\text{S}]^{2+}$  cluster to induce  $A_{\text{iso}}(^{57}\text{Fe}) \cong 2$  MHz, the exchange interaction between the radical and the closest high-spin iron center must be on the order of  $1-2 \text{ cm}^{-1}$ .<sup>10</sup> It is a relatively weak interaction that suggests no direct bonding between the iron and the carbon of the substrate. Because the intrinsic  $^{57}\text{Fe}$  HF couplings of a  $[4\text{Fe}-4\text{S}]^{2+}$  cluster are expected to be predominantly isotropic,<sup>10a,11</sup> the dipolar coupling observed is likely due to a through-space interaction between the cluster and the substrate radical. The  $A_{\text{anis}} = 0.35$  MHz observed in the current case would correspond to an effective dipole-dipole distance between the unpaired spin on the substrate and the  $^{57}\text{Fe}$  nucleus distance of 2.0 Å. Although, this distance likely does not represent an actual geometric distance between a carbon of the substrate and an  $^{57}\text{Fe}$  nucleus of the  $[4\text{Fe}-4\text{S}]$  cluster, this calculation does place the substrate-based radical in an extreme close proximity to one of the  $[4\text{Fe}-4\text{S}]$  clusters of LipA.

As it has been shown that the auxiliary cluster donates sulfur atoms during turnover,<sup>7</sup> we suggest that the interaction observed in this work is between the substrate radical and the auxiliary cluster. Furthermore, according to the evidence obtained earlier, it is most likely that the substrate closely interacts with one of the bridging sulfur atoms rather than with the iron atoms in the  $[4\text{Fe}-4\text{S}]$  cluster to allow efficient transfer of the sulfur to the substrate during turnover. Our present data are consistent with this hypothesis. Although the dipolar distance deduced from the anisotropy of the  $^{57}\text{Fe}$  hyperfine interaction is extremely short, our analysis of the isotropic interaction shows surprisingly weak exchange coupling. The conundrum can be resolved if we assume that C4 and C6 are closely interacting with or binding to the bridging sulfur atoms of the  $[4\text{Fe}-4\text{S}]$  cluster. This will place the unpaired-spin-bearing C5 site closer to the Fe atoms, but due to the lack of spin density on C4 and C6, exchange interactions between the spin systems is expected to be weak. This scenario is supported by the  $\text{sp}^3$ -like character of the  $^1\text{H}$  HF coupling constants observed for C4 and C6.

To summarize, the data presented in this report provide direct experimental evidence of the H protein-based substrate radical and its close-range interaction with the auxiliary  $[4\text{Fe}-4\text{S}]$  cluster. Therefore, the obtained results confirm the first part of the proposed mechanism, in which formation of a cross-linked species initiates the oxidation of one of the bridging  $\mu$ -sulfido ions, which in turn results in the loss of one of the iron ions and addition of the sulfur atom to the substrate carbon.

## ■ ASSOCIATED CONTENT

### 📄 Supporting Information

The Supporting Information is available free of charge on the ACS Publications website at DOI: 10.1021/jacs.5b04387.

Experimental methods, supplementary figures, and results (PDF)

## ■ AUTHOR INFORMATION

### Corresponding Authors

\*squire@psu.edu

\*alexey.silakov@gmail.com

### Notes

The authors declare no competing financial interest.

## ■ ACKNOWLEDGMENTS

This work was supported by NIH Grants GM-63847 and GM-103268 (S.J.B.) and Tobacco Settlement Funds (TSF13/14 SAP 4100062216) to S.J.B. We thank Michael T. Green for access to instrumentation supported by NIH grant GM-101390 (M.T.G.). Mass spectrometric analyses were performed at the Penn State Proteomics and Mass Spectrometry Core Facility, University Park, PA.

## ■ REFERENCES

- (1) (a) Krest, C. M.; Onderko, E. L.; Yosca, T. H.; Calixto, J. C.; Karp, R. F.; Livada, J.; Rittle, J.; Green, M. T. *J. Biol. Chem.* **2013**, *288*, 17074–17081. (b) van der Donk, W. A.; Krebs, C.; Bollinger, J. M., Jr. *Curr. Opin. Struct. Biol.* **2010**, *20*, 673–683.
- (2) Wang, S. C.; Frey, P. A. *Trends Biochem. Sci.* **2007**, *32*, 101–110.
- (3) (a) Frey, P. A.; Hegeman, A. D.; Ruzicka, F. J. *Crit. Rev. Biochem. Mol. Biol.* **2008**, *43*, 63–88. (b) Broderick, J. B.; Duffus, B. R.; Duschene, K. S.; Shepard, E. M. *Chem. Rev.* **2014**, *114*, 4229–4317.
- (4) Sofia, H. J.; Chen, G.; Hetzler, B. G.; Reyes-Spindola, J. F.; Miller, N. E. *Nucleic Acids Res.* **2001**, *29*, 1097–1106.
- (5) (a) Cicchillo, R. M.; Iwig, D. F.; Jones, A. D.; Nesbitt, N. M.; Baleanu-Gogonea, C.; Souder, M. G.; Tu, L.; Booker, S. J. *Biochemistry* **2004**, *43*, 6378–6386. (b) Douglas, P.; Kriek, M.; Bryant, P.; Roach, P. L. *Angew. Chem., Int. Ed.* **2006**, *45*, 5197–5199.
- (6) Cicchillo, R. M.; Booker, S. J. *J. Am. Chem. Soc.* **2005**, *127*, 2860–2861.
- (7) Lanz, N. D.; Pandelia, M.-E.; Kakar, E. S.; Lee, K.-H.; Krebs, C.; Booker, S. J. *Biochemistry* **2014**, *53*, 4557–4572.
- (8) Harmer, J. E.; Hiscox, M. J.; Dinis, P. C.; Fox, S. J.; Iliopoulos, A.; Hussey, J. E.; Sandy, J.; Van Beek, F. T.; Essex, J. W.; Roach, P. L. *Biochem. J.* **2014**, *464*, 123–133.
- (9) Schweiger, A.; Jeschke, G. *Principles of Pulse Electron Paramagnetic Resonance*; Oxford University Press: New York, 2001.
- (10) (a) Xia, J.; Hu, Z.; Popescu, C. V.; Lindahl, P. A.; Münck, E. *J. Am. Chem. Soc.* **1997**, *119*, 8301–8312. (b) Bominaar, E. L.; Hu, Z.; Muenck, E.; Girerd, J.-J.; Borshch, S. A. *J. Am. Chem. Soc.* **1995**, *117*, 6976–6989.
- (11) Silakov, A.; Reijerse, E. J.; Lubitz, W. *Eur. J. Inorg. Chem.* **2011**, *2011*, 1056–1066.